

Turbulent particle transport driven by ion and electron modes

A. Skyman¹, H. Nordman¹, J. Anderson¹, L. Fazendeiro¹, P. Strand¹, D. Tegnered¹, R. Singh²

¹ Department of Earth and Space Sciences, Chalmers University of Technology, Gothenburg, Sweden

² Institute for Plasma Research, Bhat, Gandhinagar, Gujarat, India

Introduction

The topic of the present work is the turbulent transport of main ions and impurities driven by ion modes (ITG) and electron modes (TE and electron scale ETG). Particle transport in regions relevant to the pedestal region of H-mode plasmas, i.e. with steep density gradients, are of particular interest. Using the code GENE [1, 2]¹, quasi- and nonlinear gyrokinetic simulations are performed, and the results are compared with a computationally efficient fluid model [3].

The transport properties are quantified by locally finding density gradients (R/L_n) yielding zero particle flux, which are directly related to the balance of convective and diffusive transport. This measure of the impurity peaking is calculated for ITG and TE mode turbulence in source-free regions of the plasma, and scalings are obtained for the driving gradients and the impurity charge number (Z). Further, the quality of the helium ash removal is studied for ITG and TE mode drive turbulence. For ETG modes, the focus is on the main ion transport, and the density gradient leading to zero main ion particle flux, related to the formation and sustainment of the edge pedestal, is estimated.

Theoretical background

The particle transport for species j is derived from

$$\Gamma_j = \langle \delta n_j v_{E \times B} \rangle = -D_j \nabla n_j + n_j V_j \quad (1)$$

where Γ_j is the particle flux and n_j the density of the species, and $\langle \cdot \rangle$ means a spatial averaging [4, 5]. On the right hand side of Eq. (1), the transport has been divided into a diffusive and a convective part. For the domain studied ∇n_j and ∇T_j are constant ($-\nabla n_j/n_j = 1/L_{n_j}$ and $-\nabla T_j/T_j = 1/L_{T_j}$). The flux can therefore be written

$$\frac{R\Gamma_j}{n_j} = D_j \frac{R}{L_{n_j}} + R V_j, \quad (2)$$

with R the major radius of the tokamak.

In the core region of the tokamak, convection (“pinch”) and diffusion balance to give zero flux in steady state. The *zero flux peaking factor* quantifies this

$$0 = D_j \frac{R}{L_{n_j}} + R V_j \Leftrightarrow -\frac{R V_j}{D_j} \Big|_{\Gamma_j=0} = \frac{R}{L_{n_j}} \Big|_{\Gamma_j=0} \equiv P F_j \quad (3)$$

¹See <http://gene.rzg.mpg.de/> for details on the GENE code

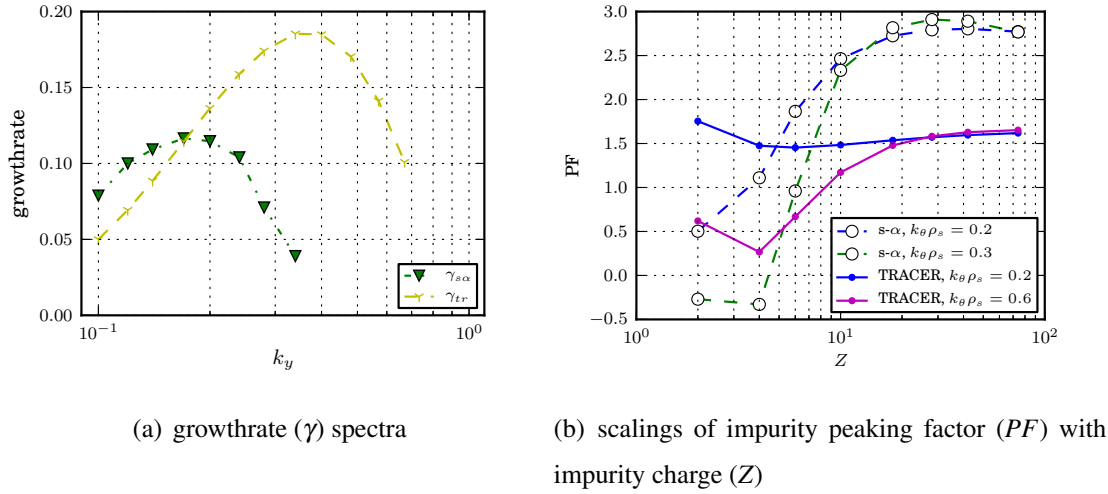


Figure 1: Comparison of s- α and realistic geometry for ITG dominated case with JET-like parameters.

Thus PF_j is interpreted as the *gradient of zero particle flux*. For trace impurities D_Z and V_Z are independent of ∇n_Z . Eq. (2) is then linear in R/L_{n_Z} , and PF_Z can be found by fitting a straight line to flux data. In general, however, D_j and V_j may depend on ∇n_j , and PF_j has to be found explicitly from the zero flux condition.

Effects of realistic geometry on ITG turbulence

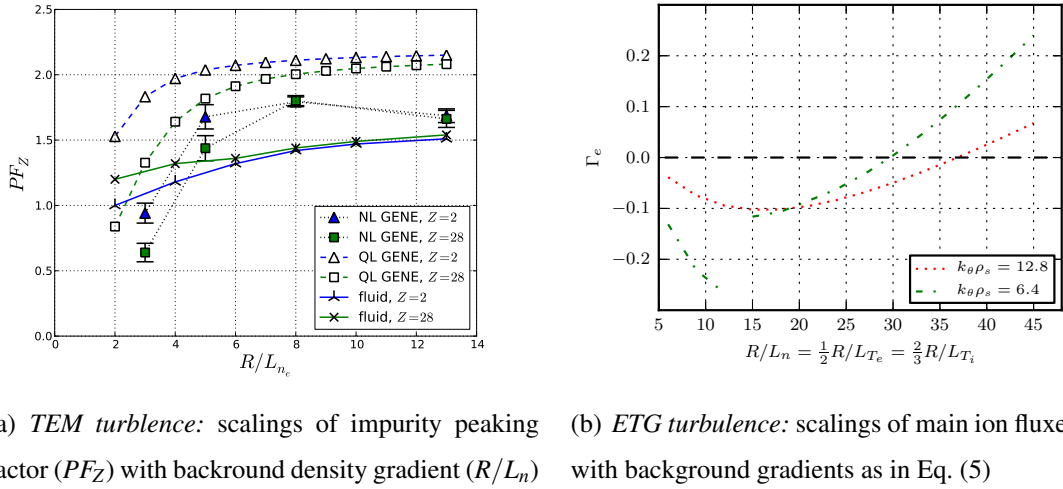
Simulations of impurity transport using a realistic *JET*-like magnetic equilibrium were compared to s- α -geometry for an ITG dominated discharge. Parameters were chosen to correspond closely to *JET L-mode discharge #67730*, with $\hat{s} = 0.8$, $q = 2.2$, $R/L_n = 2.7$, $R/L_{T_{i,e}} = 5.6$, and elongation $\kappa = 1.37$ at $r/a = 0.5$.

As shown in Fig. 1(a), with the realistic geometry the growthrate spectrum is destabilised, and shifted towards higher $k_\theta \rho_s$. This is due to a modification of curvature and FLR effects in non-circular geometry, mainly due to elongation, and is consistent with the fluid results in [6].

Weaker scalings of PF_Z with Z were consistently observed, and the level at which PF_Z saturates for high Z was reduced in the realistic case; see Fig. 1(b). The lower levels can be attributed to a reduction of the curvature pinch due the changed geometry. A large increase in PF_Z was observed for the He impurity in the realistic case. This is due to a change in sign of the (outward) thermopinch for low Z in the realistic case. NL and QL impurity pinch qualitatively agree with results in [5, 7].

The efficient removal of the He ash requires $\tau_E/\tau_{He} \geq 0.15$ [8]. This confinement time ratio can be estimated by $D_{He,eff}/\chi_{eff}$, where for $T_e = T_i$ we have:

$$\chi_{eff} = \frac{\chi_e R/L_{T_e} + \chi_i R/L_{T_i}}{R/L_{T_e} + R/L_{T_i}}. \quad (4)$$



(a) *TEM turbulence*: scalings of impurity peaking factor (PF_Z) with background density gradient (R/L_n) (b) *ETG turbulence*: scalings of main ion fluxes (Γ_e) with background gradients as in Eq. (5)

Figure 2: Scalings with background gradients for TE and ETG mode dominated cases.

For a simple comparison between different cases an estimate of D_{He}/χ_{eff} is sufficient [7]. Results from NL GENE simulations indicate that TEM turbulence is at least as efficient as ITG mode turbulence at removing He ash for the parameters studied, and that the pump out is more efficient in the realistic case; see Tab. 1.

Table 1: Estimates of helium pump out from NL GENE data

	χ_{eff}^\dagger :	D_{He}^\dagger :	D_{He}/χ_{eff} :
ITG (s- α) [5, 7]:	-	-	1.0
TE (s- α) [7]:	-	-	1.7
ITG (TRACER):	4.4	9.7	2.2

† : gyrobohm units

Steep gradients in TE and ETG mode dominated turbulence

Simulations were performed of steep density gradients where TE mode turbulence dominates, with $\hat{s} = 0.8$, $q = 1.4$, $R/L_n \in [2.0, 13.0]$, $R/L_{T_i} = 3.0$, $R/L_{T_e} = 7.0$ at $r/a = 0.4$.

It was observed that NL and QL peaking factors saturate at $PF_Z \sim 2$ for steep gradients, as the diffusion is balanced by the inward pinch; see Fig. 2(a). In contrast, the linear TEM growthrate (γ) increases uniformly with the background gradients. The peaking of impurities is weaker than the background gradient for $R/L_{n_e} \gtrsim 2$. The fluid and gyrokinetic results agree well.

For ETG modes the focus is on the density gradient leading to zero main ion particle flux, related to the formation and sustaining of the edge pedestal. The parameters are chosen to

correspond to barrier like parameters for *ASDEX Upgrade* [9], with

$$R/L_n = \frac{1}{2}R/L_{T_e} = \frac{2}{3}R/L_{T_i} \in [5.0, 45.0], \quad (5)$$

and $\hat{s} = 1.0$, $q = 3.0$ at $r/a = 0.9$.

Zero particle flux for the background was observed at very steep gradients for $k_\theta \rho_s$ consistent with ETG mode turbulence; see Fig. 2(b). This is in line with fluid results in **I1.103**. For ETG fluctuation and transport level estimates see **P2.061** and **I1.103**.

Acknowledgements

The simulations were performed on resources provided on the Lindgren² and HPC-FF³ high performance computers, by the Swedish National Infrastructure for Computing (SNIC) at Parallelldatorcentrum (PDC) and the European Fusion Development Agreement (EFDA), respectively.

The authors would also like to thank F. Jenko, T. Görler, F. Merz, M. J. Püschel, D. Told, and the rest of the GENE team at IPP–Garching for their valuable support and input.

References

- [1] F. Jenko, W. Dorland, M. Kotschenreuther, and B. N. Rogers. Electron temperature gradient driven turbulence. *Phys. Plasmas*, 7(5):1904, 2000.
- [2] F. Merz. *Gyrokinetic Simulation of Multimode Plasma Turbulence*. Ph.d. thesis, Westfälischen Wilhelms-Universität Münster, 2008.
- [3] J. Weiland. *Collective Modes in Inhomogeneous Plasmas*. IoP Publishing, 2000.
- [4] C. Angioni and A. G. Peeters. Direction of impurity pinch and auxiliary heating in tokamak plasmas. *Phys. Rev. Lett.*, 96:095003, 2006.
- [5] H. Nordman, A. Skyman, P. Strand, C. Giroud, F. Jenko, F. Merz, V. Naulin, T. Tala, and the JET-EFDA contributors. Fluid and gyrokinetic simulations of impurity transport at JET. *Plasma Phys. Contr. F.*, 53(10):105005, 2011.
- [6] J. Anderson, H. Nordman, and J. Weiland. Effects of non-circular tokamak geometry on ion-temperature-gradient driven modes. *Plasma Phys. Contr. F.*, 42(5):545, 2000.
- [7] A. Skyman, H. Nordman, and P. Strand. Impurity transport in temperature gradient driven turbulence. *Phys. Plasmas*, 19(3):032313, 2012. URL [arXiv:1107.0880](https://arxiv.org/abs/1107.0880).
- [8] D. Reiter, G. H. Wolf, and H. Kever. Burn condition, helium particle confinement and exhaust efficiency. *Nucl. Fusion*, 30(10):2141, 1990.
- [9] D. Told, F. Jenko, P. Xanthopoulos, L. D. Horton, E. Wolfrum, and ASDEX Upgrade team. Gyrokinetic microinstabilities in ASDEX Upgrade edge plasmas. *Phys. Plasmas*, 15(10):102306, 2008.

²See <http://www.pdc.kth.se/resources/computers/lindgren/> for details on Lindgren

³See <http://www2.fz-juelich.de/jsc/juropa/> for details on HPC-FF